Journal of Oceanography, Vol. 66, pp. 801 to 813, 2010

Lagrangian Observation of Phytoplankton Dynamics at an Artificially Enriched Subsurface Water in Sagami Bay, Japan

Takako Masuda[1]*, Ken Furuya[1], Naoko Kohashi[1†], Mitsuhide Sato[1], Shigenobu Takeda[1††], Makoto Uchiyama[2], Naho Horimoto[2] and Takashi Ishimaru[2]

[1]*Department of Aquatic Bioscience, The University of Tokyo, Yayoi, Bunkyo-ku, Tokyo 113-8657, Japan*
[2]*Department of Marine Sciences, Tokyo University of Marine Science and Technology, Konan, Minato-ku, Tokyo 108-8477, Japan*

(Received 29 July 2009; in revised form 6 October 2010; accepted 6 October 2010)

Phytoplankton dynamics in the lower euphotic zone were observed by tracking a subsurface water released at 20-m depth from *Takumi*, an artificial upwelling device. *Takumi* continually discharged seawater pumped up from a depth of 205 m: this water was mixed with 5-m depth water to adjust the density to that of 20-m depth water of Sagami Bay, Japan. The discharged water was pulse-labeled at *Takumi* with uranine and tracked for 63.9 h with a drifting buoy equipped with a drogue at 20-m depth. We present a simple model to estimate *in situ* phytoplankton net growth rates from temporal changes in phytoplankton abundance in the discharged water with correction for the influence of water exchange between the discharged water and neighboring layers. Lagrangian observation showed active growth of pico- and nanophytoplankton, especially cryptophytes and *Synechococcus* (Cyanobacteria), in the subsurface layer. In contrast, diatoms grew little in spite of micromolar concentrations of nutrients. The active growth of pico- and nanophytoplankton was in good agreement with shipboard serial dilution culture experiments. The low growth activity of diatoms was suggested to be related to low light availability in the subsurface layer.

Keywords:
· Phytoplankton growth,
· Lagrangian observation,
· serial dilution culture.

1. Introduction

Subsurface chlorophyll maximum (SCM), or deep chlorophyll maximum, is a common feature of the vertical distribution of chlorophyll *a* (Chl *a*) in stratified water columns over continental shelves (Cullen and Eppley, 1981) or in the open ocean (Saijo *et al*., 1969). The SCM is usually located in the vicinity of a maximum water density gradient and tends to be associated with the nitracline (Cullen and Eppley, 1981). Ecological implications of the SCM vary widely depending on locations and season. At some locations, the SCM is an important element of primary production, particularly new production (Richardson *et al*., 2000; Sharples *et al*., 2001; Weston *et al*., 2005) suggesting that the phytoplankton community in the SCM captures upward nutrient fluxes from the water layer below the euphotic zone. However, the growth activity of phytoplankton in the SCM is not well understood.

Diatoms are often the dominant phytoplankton in natural waters with sufficient nitrate supply at micromolar concentrations during spring blooms (Parsons *et al*., 1984) or in upwelling regions (Ryther, 1969; Ishizaka *et al*., 1983; Furuya *et al*., 1986). In particular, chain-forming centric groups exhibit active growth. However, the ample availability of nitrate does not necessarily allow diatom dominance as seen in subsurface assemblages in stratified water where the SCM is mainly composed of pico- and nanophytoplankton other than diatoms (Furuya and Marumo, 1983; Furuya, 1990; Richardson *et al*., 2000; Sharples *et al*., 2001; Weston *et al*., 2005).

Growth of SCM phytoplankton has been measured by bottle incubation procedures (Furuya, 1990; Obayashi

* Corresponding author. E-mail: amasuda@mail.ecc.u-tokyo.ac.jp

† Present address: Department of Ocean Civil Engineering, Kagoshima University, Korimoto, Kagoshima 890-0065, Japan.
†† Present address: Faculty of Fisheries, Nagasaki University, Bunkyo, Nagasaki 852-8521, Japan.

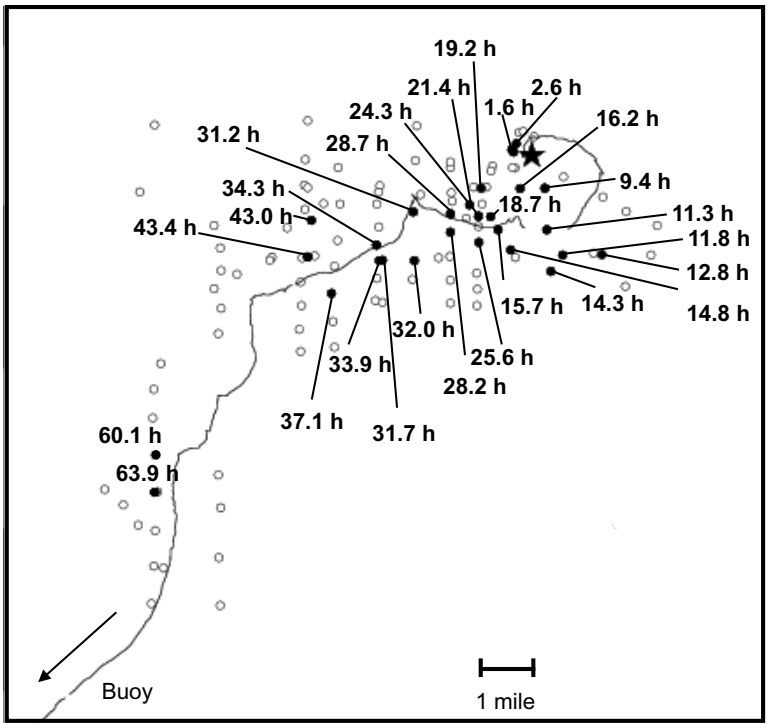

Fig. 1. Sampling locations during a buoy tracking experiment. The star and solid line denote the location of *Takumi* and buoy trajectory, respectively. Open circles indicate stations for CTD casts. Closed circles denote stations for water sampling, with which time after the start of the buoy tracking is indicated.

and Tanoue, 2002; Selph *et al*., 2005). However, bottle incubations containing natural populations are subject to the so-called "bottle effect", in which the longer a seawater sample is confined in a bottle, the more marked are the changes in plankton composition (Venrick *et al*., 1977). In contrast, rates obtained from temporal changes in abundance of *in situ* assemblages are conceptually simple and free from possible artifacts associated with containing populations in artificial enclosures. However, such a Lagrangian approach presents various challenges including (1) the difficulty of detecting *in situ* a unique water mass over an adequate time period; (2) the complex spatio-temporal variability in fluid movements (Basterretxea *et al*., 2002; Mariano *et al*., 2002); and (3) the requirement for an interdisciplinary oceanographic approach to synthesize physical, chemical, and biological processes of interest. To our knowledge, no attempt has been made to date to apply the Lagrangian approach to estimate phytoplankton growth in the lower part of the euphotic zone due to challenge (1). Furthermore, challenge (2) makes estimation of phytoplankton growth in a given water layer extremely complex.

In the present study, we estimated growth rates of an *in situ* phytoplankton assemblage in a subsurface layer by time-series monitoring of algal abundances based on *in situ* Lagrangian observation. *In situ* growth was compared with rates obtained by shipboard *in vitro* incubations. Lagrangian observations involved tracking a uranine-labeled subsurface water released from an artificial upwelling device, dubbed *Takumi* (Takahashi and Ikeya, 2003).

2. Materials and Methods

2.1 Field observations

Takumi was moored in the center of Sagami Bay (35.05°N, 139.25°E, Fig. 1); it continually pumped up 1×10^5 m^3 of deep water per day from 205-m depth and released it as a subsurface water at 20-m depth (Miyabe *et al*., 2004). Since the water from 205-m depth was sufficiently dense to sink out of the euphotic zone, we mixed it in a ratio of 1:2 with less dense water from 5-m depth within *Takumi*. The mixture was discharged from the horizontally located circular outlet of *Takumi* along an isopycnal layer at the 20-m depth (Ouchi and Omura, 2004; Ouchi *et al*., 2005). Because *Takumi* discharged the mixed water at a 20-m depth, we expected to track a subsurface population by Lagrangian observations using a drifting buoy fitted with a drogue at 20-m depth, and by uranine labeling of the discharged water.

Observation and seawater sampling were conducted around *Takumi* during the KT-06-16 cruise of R/V "Tansei-Maru" from July 28, 2006 to August 4, 2006. *Takumi* continually discharged water from May 9, 2006 onward. A subsurface discharged water produced in this manner was labeled with uranine from 11:00 to 11:17 JST on July 30. The tracer was added to the chamber in *Takumi* in which waters from 5-m and 205-m depth were mixed and then released. Times of observation and sampling refer to elapsed hours (h) after 11:08 JST on July 30, the midpoint of the dye-marking period. After the discharged water was labeled, a drifter fitted with a drogue at a 20-m depth and a global positioning system (GPS) transmitter at the surface were immediately deployed near *Takumi* and tracked for 63.9 h. During tracking, we conducted vertical water profiling procedures every 15 min in the upper 50-m water column near the buoy using a conductivity, temperature, and depth (CTD) device (FSI, Cataumet, MA) fitted with an underwater fluorometer tuned for uranine (Dr. Haardt, Kleinbarkau, Germany). Water samples for uranine measurement were collected at 27 stations (Fig. 1) with Niskin bottles placed on a rosette array fitted with the CTD profiler. Water samples for nutrients, phytoplankton pigments, and cell densities were collected at 2.6, 9.4, 24.3, 28.8, 34.3, 43.4, and 63.9 h across the 27 stations. Uranine concentrations were monitored with an underwater fluorometer and with a shipboard fluorometer for discretely sampled water. Samples of nutrients were immediately frozen without filtration and later analyzed for nitrate, nitrite, and phosphate with an Autoanalyzer (TRAACS2000; Bran+Luebbe) on land. Surface light irradiance was measured with a Biospherical QSP-200 (4π collector) irradiance sensor. The irradiance in the discharged water layer was calculated from the vertical attenuation coefficient estimated from the vertical distribution of Chl *a* (Riley, 1946). We evaluated the Kyucho (Matsuyama *et al*., 1999) from sea surface temperature images provided by NASA's MODIS/AQUA (http://oceancolor.gsfc.nasa.gov/).

2.2 Phytoplankton analysis

For pigment analyses by high-performance liquid chromatography (HPLC), 1-L subsamples from the Niskin bottles were transferred into high-density polyethylene opaque bottles and vacuum filtered onto GF/F filters under a gentle suction (<150 mmHg). The filters were kept in liquid nitrogen until analysis. Frozen filters were soaked in 95% methanol and sonicated for 5 min; subsequently, the filtrate was allowed to settle for 60 min at 4°C. Pigments in the extracts were separated through a reverse-phase C_8 column using a dual solvent high-pressure gradient protocol (Zapata *et al*., 2000). Carotenoids and chlorophylls were identified and quantified with a photodiode array detector (SPD-M10AV; Shimadzu, Japan) by comparing their retention times and absorbance spectra with those obtained from commercial standards (Water Quality Institute, Denmark). Pigment composition and concentrations were interpreted using the CHEMTAX program (Mackey *et al*., 1996, 1997) to obtain class-specific composition of Chl *a*. An initial ratio matrix was adapted from that of Hashihama *et al*. (2008).

Additional 5-mL aliquots of the subsamples were preserved in glutaraldehyde at a final concentration of 1% (v/v) for flow cytometry, snap-frozen in liquid nitrogen, and stored in a deep-freezer at –80°C until analysis on land. We used a flow cytometer (PASIII; Partec, Germany) equipped with 10-mW argon ion lasers. The sample flow rate and fluorescence intensity were calibrated with a mixture of 0.5-, 1.0-, and 2.0-μm green fluorescent polystyrene beads (Polysciences, USA). Forward- and side-angle light scatters (FSCs and SSCs) and fluorescence events were collected as a list mode, saved, and analyzed with FloMax software (Partec, Germany). The cyanobacterium *Synechococcus*, pico- and nanoeukaryotes, and cryptophytes were distinguished from one another by their light scattering and auto-fluorescence properties.

2.3 Serial dilution culture

Phytoplankton growth and zooplankton grazing rates were estimated from serial dilution cultures during buoy tracking (Landry and Hassett, 1982). Incubations were conducted twice using water samples collected at 21.4 h (experiment (A)) and 42.9 h (experiment (B)) after tracer labeling. Water samples were collected from the discharged water layer, which was identified as the layer with the highest concentration of uranine during vertical profiling. To determine the relationship between pico- and nanophytoplankton and heterotrophic nanoflagellates, we sieved subsamples through a 200-μm mesh to remove larger particles. In addition, almost half of the <200-μm filtrate was filtered through a GF/F filter. A dilution series of 100%, 70%, 40%, and 10% of the <200-μm subsample was prepared in triplicate with the GF/F filtrate, and then incubated in 1-L polycarbonate bottles for 24 h in a shipboard incubator. To simulate light conditions in the subsurface layer, light intensity in the bottles was adjusted to 9% of surface value using neutral density screens. Temperature was maintained constant using a thermostat circulator. Chl *a* and cell densities of pico- and nanophytoplankton were determined at the start and end of incubations by fluorometric measurements on *N*,*N*-dimethylfolmamide extracts of Chl *a* (Suzuki and Ishimaru 1990), and flow cytometry, respectively.

Phytoplankton net growth rates at each dilution level (μ_i) were defined as follows:

$$\mu_i = 1/t \ln\left(N_t / N_0\right) \quad (1)$$

where N_0 and N_t are initial and final concentrations of Chl *a* or cell densities, respectively, and t is the duration of incubations.

Second, phytoplankton gross growth (k) and grazing rate (g) were calculated according to Landry and Hassett (1982):

$$\mu_i = k - gD_i \quad (2)$$

where, μ_i is the observed rate of net growth, as mentioned above, and D_i is the dilution level.

Third, ambient net growth rate (μ) was estimated from the difference between the computed values of k and g (Landry *et al*., 1993):

$$\mu = k - g \quad (3)$$

2.4 Photodecomposition of uranine

Because uranine is known to photodecompose, quantities of decomposition products were estimated during the observation using the attenuation coefficient of –0.135 mol photon^{-1} m^2 (Ikeya *et al*., 2009). The uranine concentration of the discharged water at 2.6 h, obtained at the first station, was designated the initial uranine concentration and was assumed to photodecompose with time depending on the total quantity of photons at 20-m depth from 2.6 h onward to the point in time of interest. Decomposed uranine amounts were added to observed concentrations at every 0.5 h interval. In this calculation, we used the extinction coefficient of underwater photosynthetically active radiation (PAR) obtained at *Takumi* and the temporal change in surface incident light recorded in the central part of Tokyo Bay.

2.5 Phytoplankton net growth rate by Lagrangian observation

First, in order to evaluate the mixing between layers, an "entrainment velocity" (Fischer *et al*., 1979) was calculated from the observed uranine concentrations as follows:

$$D\left(\overline{C_{in}}l\right)\Big/Dt = \left(\overline{C_{out}} - \overline{C_{in}}\right)W_e \quad (4)$$

where $\overline{C_{in}}$ and $\overline{C_{out}}$ are the mean uranine concentrations within and outside the discharged water respectively, estimated after spline interpolation, and l is the thickness of the discharged water. D/Dt and W_e are Lagrangian derivative and the entrainment velocity, respectively. W_e is defined as the contribution of vertical mixing including vertical diffusion and is proportional to the gradient of uranine concentrations. Since *Takumi* released water in all directions horizontally, we assume horizontal variations in uranine concentration were negligibly small compared with its vertical change. Then, effects of horizontal mixing on uranine concentration were ignored in the present study. Equation (4) was derived on the basis of the assumption that the shape of the discharged water was axially symmetrical, because the vertical profiles of uranine were consistently symmetrical around the uranine maximum. Thus, $\overline{C_{out}}$ was assumed to be equal for both the layers above and below the discharged water. The left-hand side of Eq. (4) is approximated by the following finite differential method:

$$D\left(\overline{C_{in}}l\right)\Big/Dt \approx \Delta\left(\overline{C_{in}}l\right)\Big/\Delta t \quad (5)$$

Subsequently, net growth rates of phytoplankton in the discharged water were estimated from the Chl *a* levels for total assemblages and flow cytometric cell counts for pico- and nanoplankton. Influences of vertical mixing of discharged water with outside water were eliminated with the following equation:

$$D\left(\overline{P_{in}}l\right)\Big/Dt \approx \Delta\left(\overline{P_{in}}l\right)\Big/\Delta t = \left(\overline{P_{out}} - \overline{P_{in}}\right)W_e + \mu\overline{P_{in}}l \quad (6)$$

where $\overline{P_{in}}$, $\overline{P_{out}}$, and μ are mean phytoplankton abundance within and outside the discharged water, and net growth rate during a time period Dt, respectively. $\overline{P_{in}}$ and $\overline{P_{out}}$ were estimated using weighted average.

3. Results

3.1 Hydrographic conditions

The study area was stratified with less saline (<33.6) and warm (>20°C) water lying in the top 15-m layer, and a pycnocline was located around a 20-m depth until 63.9 h. The temperature at 10-m depth suddenly increased from 19.6 ± 0.8 to 20.8 ± 1.3°C at 41.3 h ($p < 0.01$). The buoy moved along a clockwise trajectory at a velocity of 287 ± 99 m h^{-1} during the first 28 h, and then shifted to the southwest (Fig. 1). At 41.3 h, buoy velocity increased suddenly to 620 ± 166 m h^{-1}. Sudden high velocity intrusions of warm water from the Kuroshio near the coastline of Sagami Bay are well known as Kyucho (sudden, rapid movements of water). We observed extensive intrusion of warm water into Sagami Bay. The water under observation probably came under Kyucho influence at 41.3 h. After the Kyucho occurred, the speed of the buoy increased further, and it moved more rapidly toward the southwest. The estimated irradiance at the 20-m depth ranged from 44 to 117 μmol photons m^{-2}s^{-1} (corresponding to 6 ± 3% of surface photon irradiance).

3.2 Temporal changes in the distribution of uranine and nutrients

The vertical maximum uranine concentration was

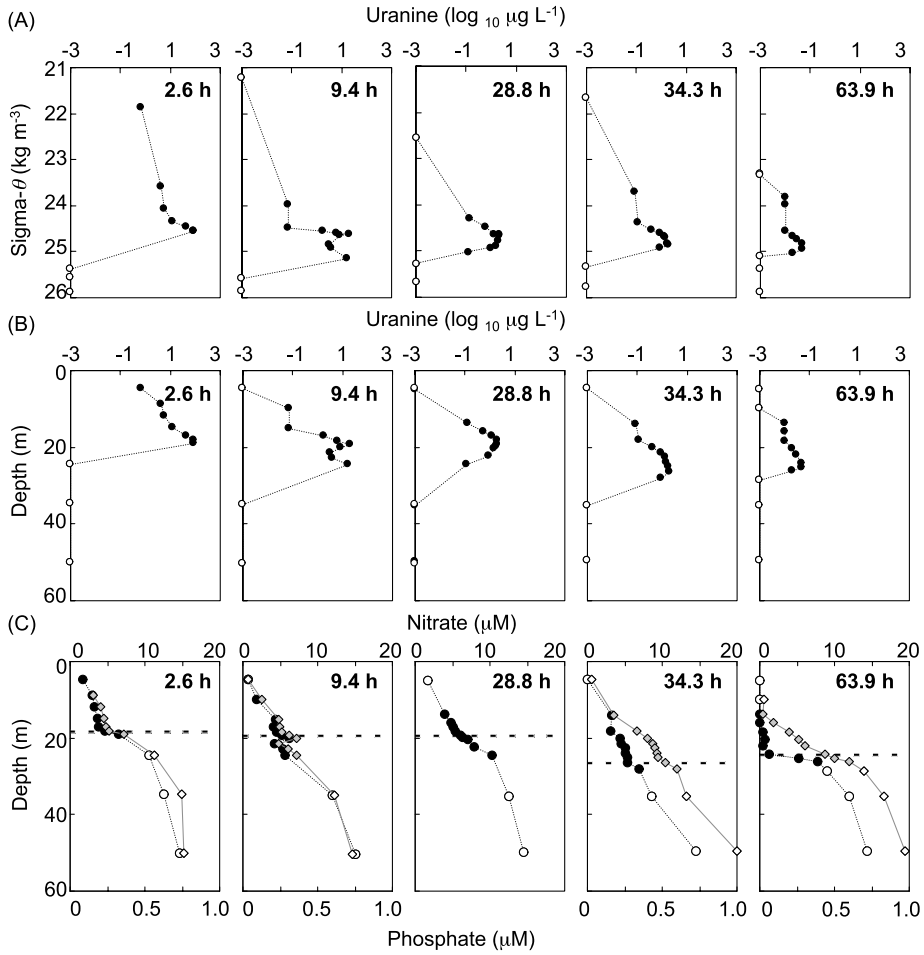

Fig. 2. Vertical distribution of (A), (B) uranine and (C) nitrate (circle) and phosphate (diamond) at selected stations indicated by closed circles in Fig. 1. (A) and (B) are vertical uranine distributions against sigma-θ and depth, respectively. Closed circles and opaque diamonds denote layers where uranine was detected, while open ones denote layers where uranine was not detected (<0.01 mg L^{-1}). Dashed lines represent the discharged water layer as determined by the vertically maximum concentrations of uranine.

highest in a water sample collected at 2.6 h (87.06 μg L^{-1}): it decreased steadily with time to 0.05 μg L^{-1} at 63.9 h (Fig. 2). The depth where the maximum uranine concentration was detected varied around 18.3–25.1 m (Fig. 2). Probably due to internal waves, sigma-θ at the uranine maximum layer was relatively constant (24.5–24.7 kg m^{-3}). The initial dimensions of the discharged water, stained by uranine for 17 min, were estimated to be approximately 205 m in length, 10 m in width, and 1 m in thickness according to the current velocity at 20-m depth estimated by a shipboard ADCP (acoustic Doppler current profiler).

The initial nitrate concentrations at 5 and 205-m depths were 1.7 and 25.0 μM, respectively, at 2.6 h (Fig. 2). At 2.6 h, vertical gradients of nitrate and phosphate concentrations were steepest around the uranine maximum depth (17.1–18.9 m) from 3.9 to 6.4 and from 0.24 to 0.36 μM, respectively. This trend continued until 63.9 h (Fig. 2).

3.3 Temporal changes in the distribution of phytoplankton assemblage

Phytoplankton abundances at 5-m depth ranged from 4×10^5 cells mL^{-1} for the numerically dominant *Synechococcus* and nanoeukaryotes through 5×10^4 cells mL^{-1} for picoeukaryotes to 4×10^3 cells mL^{-1} for cryptophytes (Fig. 3). The vertical profile of *Synechococcus* at 2.6 h showed a sharp minimum (8.2×10^3 cells mL^{-1}) at the uranine maximum depth (18.3 m) and the cell density there remained low until 28.8 h (Fig. 3). Cell densities of cryptophytes, picoeukaryotes, and nanoeukaryotes were also minimal at the uranine maxi-

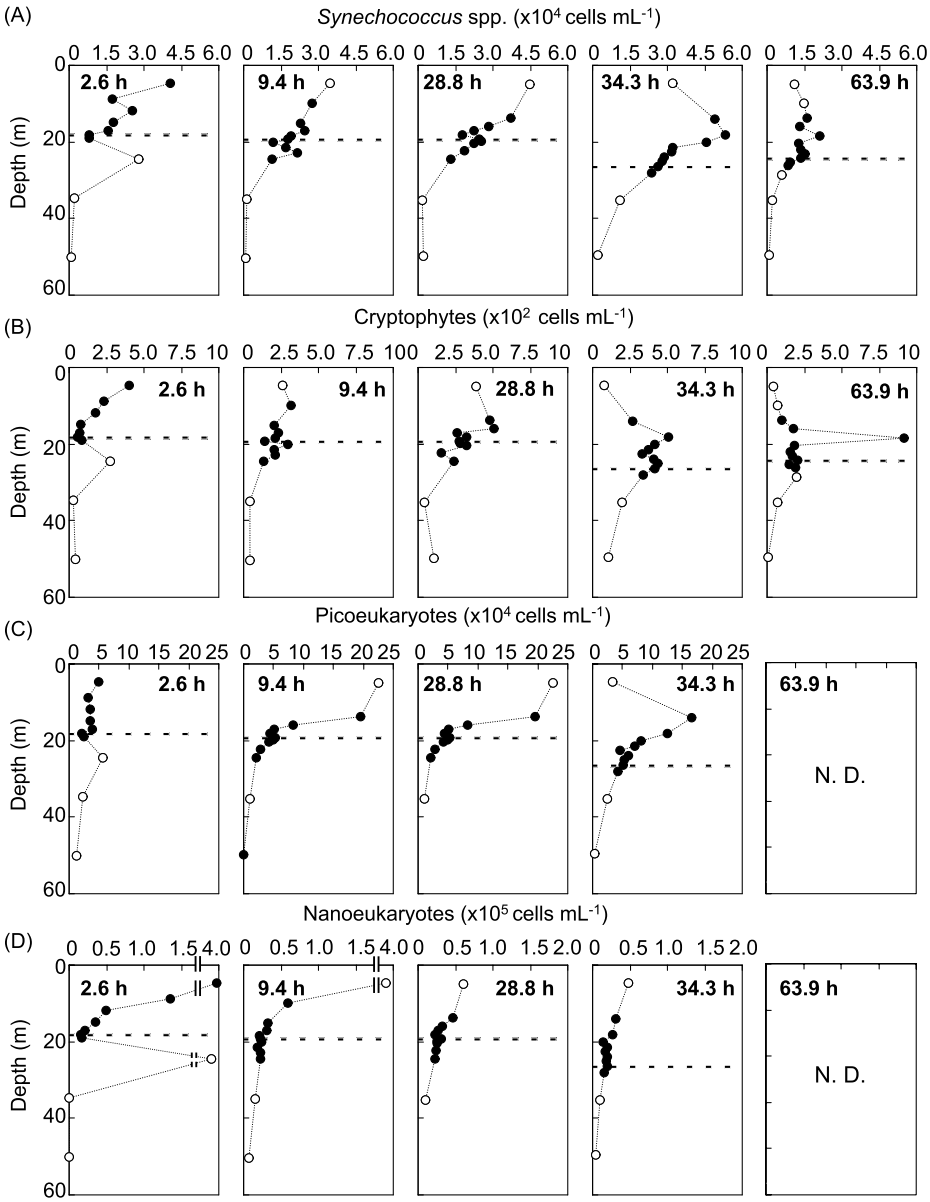

Fig. 3. Vertical distributions of (A) *Synechococcus*, (B) cryptophytes, (C) picoeukaryotes, and (D) nanoeukaryotes. Closed circles denote layers where uranine was detected, while open ones denote layers where uranine was not detected (<0.01 mg L^{-1}). Dashed lines represent the discharged water layer as determined by the vertically maximum concentrations of uranine.

mum depth, although the decrease in their densities was not as marked as that for *Synechococcus* (Fig. 3).

During the period 9.4 to 34.3 h, the SCM was observed at 17.1–24.1 m, with a maximum value of 0.70 μg L^{-1}. The Chl *a* concentration at the uranine maximum depth increased from 0.37 μg L^{-1} at 2.6 h to 0.65 μg L^{-1} at 34.3 h (Fig. 4). Initially, diatoms accounted for the major portion (43%) of total Chl *a* content: the diatom Chl *a* contribution decreased to 31% at 43.1 h (Fig. 4). At 2.6 h, prasinophytes and chlorophytes accounted for 18% and 14% of total Chl *a* content, respectively, and their contributions also decreased to 10% and 4% at 43.1 h, respectively. In contrast, the contribution of cryptophytes (8% at 2.6 h) steadily increased with time (39% at 34.4 h). During 2.6–43.1 h, the compositions of haptophytes (5–6%), dinoflagellates (2–3%), and *Synechococcus* (5–8%) remained constant (Fig. 4).

3.4 Phytoplankton growth and grazing rate estimated from serial dilution experiments

Aloricate ciliates accounted for more than 80% of the total heterotrophic plankton abundance, followed by

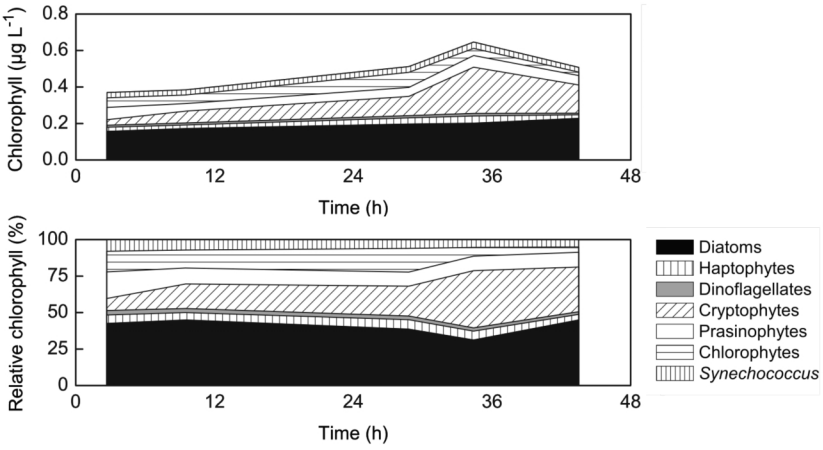

Fig. 4. Temporal changes in Chl *a* and its composition at the discharged water layer.

Table. 1. Phytoplankton growth rate and grazing rate as estimated by serial dilution culture experiments with correlation coefficient of regression analysis (r^2) of gross growth (k) and grazing rate (g), and 95% confidence interval (95% CI) for net growth rate (μ), and net growth rate (μ) estimated from Lagrangian observation. Experiments (A) and (B) were conducted within the subsurface discharged water released from *Takumi*.

Experiment	Specific rate (d^{-1})	Chlorophyll *a*	*Synechococcus*	Picoeukaryotes	Nanoeukaryotes	Cryptophytes
Serial dilution (A)	Gross growth rate (k)	0.76	1.63	1.99	1.93	1.83
	Grazing rate (g)	0.41	0.41	1.49	0.66	0.73
	Net growth rate* (μ)	0.35	1.22	0.50	1.27	1.10
	r^2	0.88	0.57	0.63	0.72	0.53
	95% CI	ND	±0.28	±0.35	±0.43	±0.62
Serial dilution (B)	Gross growth rate (k)	0.39	1.13	2.09	0.85	0.83
	Grazing rate (g)	0.13	0.78	1.71	1.11	1.68
	Net growth rate* (μ)	0.26	0.35	0.38	−0.26	−0.85
	r^2	0.61	0.78	0.87	0.81	0.84
	95% CI	ND	±0.17	±0.37	±0.24	±0.27
Lagrangian	Net growth rate** (μ)	0.51	0.95	0.53	0.47	1.11

*Estimated from serial dilution cultures.
**Estimated from the Lagrangian experiment.
ND: Not determined.

loricate ciliates and herbivorous copepods, including both nauplii and copepodites, in the initial samples for both experiments (A) and (B). Foraminiferans were not observed during both the experiments. The dilution culture procedure yielded active gross growth of *Synechococcus* (k = 1.63 and 1.13 d^{-1}), picoeukaryotes (k = 1.99 and 2.09 d^{-1}), nanoeukaryotes (k = 1.93 and 0.85 d^{-1}), and cryptophytes (k = 1.83 and 0.83 d^{-1}) (Table 1). The growth rate of phytoplankton other than picoeukaryotes was higher in the dilution experiment (A) than in the dilution experiment (B) (t-test, $p < 0.05$; Table 1). Picoeukaryotes were actively grazed in both experiments, and the grazing rate was elevated in the dilution experiment (B) (g = 1.49 and 1.71 d^{-1} for dilution experiments (A) and (B), respectively). In general, gross growth exceeded grazing, except for nanoeukaryotes and cryptophytes in dilution experiment (B).

3.5 Lagrangian estimation of phytoplankton growth rate

Phytoplankton abundance increased in the discharged water during buoy tracking (Fig. 4). This increment was the manifestation of integrals of algal growth, mortality,

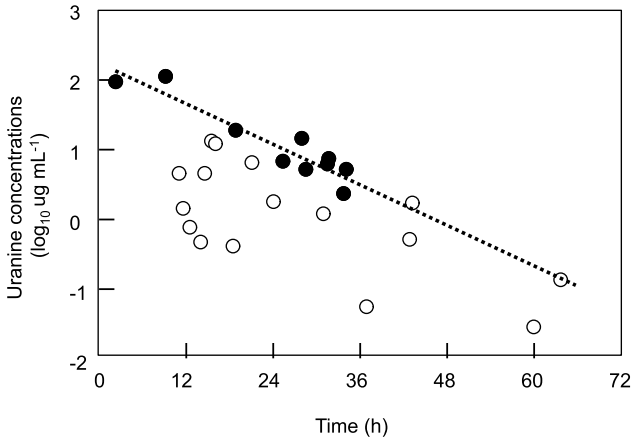

Fig. 5. Mean uranine concentrations within the discharged water ($\overline{C_{in}}$) vs. sampling time during the buoy tracking experiment (t). Dashed line shows the upper limit of the data points. Solid symbols show the data used for W_e estimation.

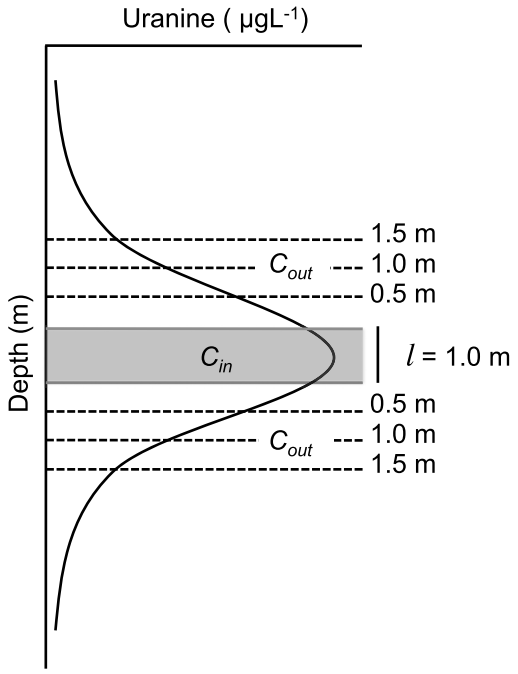

Fig. 6. Schematic illustration of a subsurface discharged water. The solid line denotes uranine concentrations. The opaque layer indicates the discharged water layer (C_{in}). Dashed lines represent the boundary of the layer outside the discharged water (C_{out}), when its thickness changes from 0.5, 1.0, and 1.5 m.

mixing with ambient waters, and sinking loss. Here, we attempted to eliminate the influences of mixing from phytoplankton abundance variation to estimate net phytoplankton growth and verify the results by comparing the data obtained by bottle incubation experiments conducted using the same water.

To overview the dynamics of uranine in the discharged water, the mean uranine concentrations within the discharged water ($\overline{C_{in}}$) during each CTD cast were plotted against time (Fig. 5). When the discharged water was poured from a 0.3 m-thick slit, discharged water thickness appeared to be greater than 0.3 m. Therefore, we examined a 1.0-m for l (Fig. 6). Because some CTD casts likely failed to capture the core of the uranine-labeled water, we considered that the upper boundary of the plots indicates a dilution curve of uranine in the discharged water core during buoy tracking. Moreover, because buoy movement remained stable during the first 41 h, we assumed that a constant value of W_e could be applied during this period. Therefore, we picked up the data obtained at 2.6, 9.4, 19.2, 24.3, 25.6, 28.8, 31.7, 32.0, 33.9, and 34.3 h for W_e estimation. Using these results, we estimated W_e from Eq. (4).

Three different thicknesses (0.5, 1.0, and 1.5 m) of $\overline{C_{out}}$ were examined (Fig. 6). Uranine concentrations at 0.5, 1.0, 1.5, and 2.0 m above and below the center of the discharged water were obtained by proportional allotment using the uranine concentrations at the uranine maximum and those in the nearest observed layer above and below the maximum, respectively (Figs. 2 and 6). The calculation using Eq. (4) yielded W_e ranging from 1.64 to 1.76 $\times$ 10^{-4} m s^{-1} (Table 2). The calculated quantity of photodecomposed uranine over 63.9 h was almost 30% of the initial concentration; photodecomposition corresponded at most to 10% of the effect of the entrainment.

Table 2. Entrainment velocity (W_e) calculated with the C_{out} thickness of 0.5, 1.0 and 1.5 m.

	Thickness of C_{out}		
	0.5 m	1.0 m	1.5 m
W_e ($\times 10^{-4}$ m s^{-1})	1.76	1.67	1.64

Subsequently, net growth rates (μ) of phytoplankton in the discharged water were estimated from Eq. (6). Chl *a* and phytoplankton cell densities at 0.5, 1.0, 1.5, and 2.0 m above or below the center were calculated by weighted average of above and below the target layer, discretely. Then, $\overline{P_{in}}$ and $\overline{P_{out}}$ in terms of Chl *a* concentration or phytoplankton cell densities were obtained.

The temporal change of $\overline{P_{in}}$ is shown in Fig. 7. Because $\overline{P_{in}}$ include the influence of growth and vertical mixing, the slope of time change of $\overline{P_{in}}$ is not directly indicative of growth rate. The mean phytoplankton abun-

dance without the influence of vertical mixing is also shown as open circles in Fig. 7, where the corrected abundance is expressed as $\overline{P_{in}^{*}}$ and $\overline{P_{out}^{*}}$. By using $\overline{P_{in}^{*}}$ and $\overline{P_{out}^{*}}$, we estimated μ from Eq. (6) (Table 1). Because of the insignificant difference in the W_e across the 3 different thicknesses of P_{out} (Table 2), the μ of phytoplankton calculated for the 3 layers outside the discharged water did not differ significantly. Hence, Table 1 shows the μ obtained for a thickness of 1 m.

The contributing ratio of vertical mixing to the increase in phytoplankton abundance in the discharged water was estimated by the following equation:

$$X = 100\left(\overline{P_{out}} - \overline{P_{in}}\right)W_e \Big/ \left\{\left(\overline{P_{out}} - \overline{P_{in}}\right)W_e + \mu\overline{P_{in}}l\right\} \quad (7)$$

where X is the ratio of contribution (%) by vertical mixing to the increase in phytoplankton abundance in the discharged water. The estimated contribution ratio varied from 0.4% to 33.4% (Table 3). The contribution ratios estimated for *Synechococcus* (33.4–3.0%), picoeukaryotes (23.3–1.2%), and nanoeukaryotes (8.1–3.6%) decreased during the period 2.6–28.8 h, and those estimated for cryptophytes continued to decrease from 29.3 to 0.8% over the period 2.6–34.4 h.

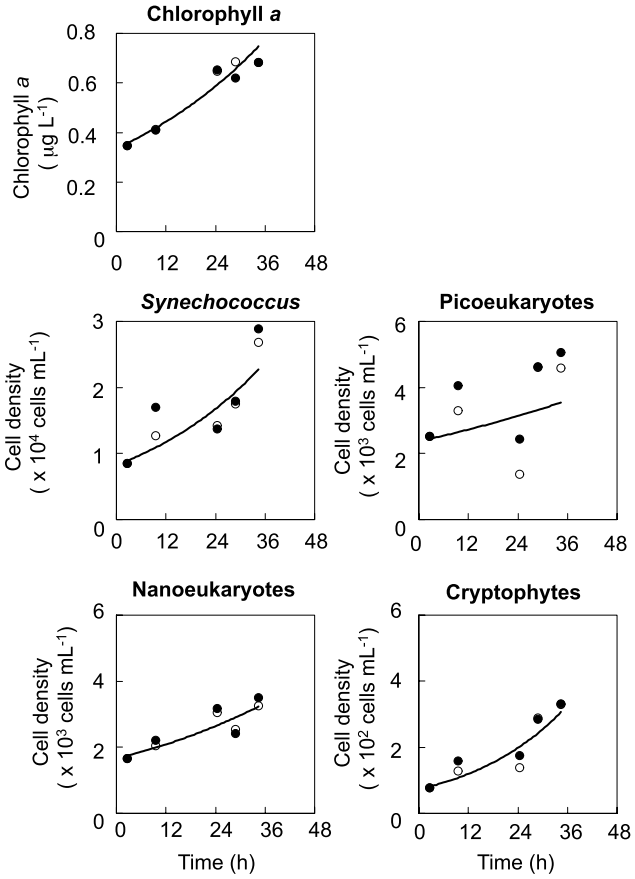

Fig. 7. Closed circles denote the temporal changes in Chl *a* concentration in the total phytoplankton population and abundance of *Synechococcus*, pico- and nanoeukaryotes, and cryptophytes at the discharged water ($\overline{P_{in}}$). $\overline{P_{in}}$ are affected with not only phytoplankton growth (μ), but also the vertical mixing effect. Open circles denote the temporal changes eliminating the influence of vertical mixing ($\overline{P_{in}^{*}}$). Solid-line shows the regression curve for $\overline{P_{in}^{*}}$.

4. Discussion

The present study is the first experiment to demonstrate the potential of Lagrangian observations in phytoplankton dynamics focusing on subsurface water layers. The methodology has been applied to surface waters in past studies (Thingstad *et al*., 2005; Boyd *et al*., 2007), where a unique water mass enriched within iron or phosphorus was successfully tracked for periods of a few days to months. In contrast, estimations of phytoplankton growth rates in subsurface layers have been limited to model calculations (Sharples *et al*., 2001; Ross and Sharples, 2007) or small incubations (Furuya, 1990; Obayashi and Tanoue, 2002; Selph *et al*., 2005). In the present study, we succeeded in tracking a subsurface water mass for almost three days by discharging density-adjusted water in the isopycnal layer with subsequent fine scale *in situ* monitoring of uranine marker concentrations (sampling resolution was close to 0.5 nautical mile). Direct monitoring of temporal changes in phytoplankton abundance enabled us to estimate phytoplankton growth rate in the subsurface layer.

Table 3. The contribution ratio of the vertical mixing to the increase in phytoplankton abundance in the discharged water, estimated from Eq. (7).

	Chlorophyll *a*	*Synechococcus*	Picoeukaryotes	Nanoeukaryotes	Cryptophytes
2.6–9.4 h (%)	0.5	33.4	23.3	8.1	29.3
9.4–24.4 h (%)	1.5	3.3	21.1	5.3	19.0
24.4–28.8 h (%)	11.0	3.0	1.2	3.6	3.0
28.8–34.4 h (%)	0.4	10.2	9.4	8.7	0.8

Table 4. Phytoplankton growth rates of subsurface phytoplankton assemblage in subtropical regions (μ, d^{-1}) estimated from changes in Chl *a* or particulate carbon concentrations during dilution experiments.

Area	Sampling depth (m)	$\%E_0$	Temperature (°C)	Growth rate (μ, d^{-1})	Reference
Western North Pacific	100	—	24.9–26.4	0.42–0.98	Furuya, 1990
Western North Pacific	20–35	10	17.4–25.3	0.38–0.54	Obayashi and Tanoue, 2002
North Pacific	55, 66	12	24.2, 24.4	0.11, 0.22	Selph *et al*., 2005
Arabian Sea	29–54	6	25.4–28.2	0.37–0.96	Landry *et al*., 1998
Arabian Sea	27–65	5	21.2–28.1	0.01–1.14	Landry *et al*., 1998
Arabian Sea	35–74	3	24.7–27.1	0.14–0.75	Landry *et al*., 1998
Equatrial Pacific	40–50	14	23.8–25.5	0.89–1.11	Landry *et al*., 1995
Equatrial Pacific	40–50	8	28.4–28.6	0.14–0.51	Landry *et al*., 1995
Equatrial Pacific	70–80	1	21.3–28.4	0.07–0.43	Landry *et al*., 1995
Equatrial Pacific	30	15	—	1.02 ± 0.22	Landry *et al*., 2003
Equatrial Pacific	60	3	—	0.59 ± 0.19	Landry *et al*., 2003
Sagami Bay	20, 21	6	19	0.35, 0.26	This study

E_0: surface irradiance.

Active photosynthesis, primary production, and nitrogen (ammonium + nitrate) uptake have been reported previously for the subsurface water layer (Takahashi *et al*., 1972, 1985; Richardson *et al*., 2000; Weston *et al*., 2005). In this layer, picophytoplankton (*ca*. <3 μm) (Furuya, 1990), particularly *Synechococcus*, and dinoflagellates (Weston *et al*., 2005; Hickman *et al*., 2009) are dominant. In addition, diatoms are occasionally dominant (Hickman *et al*., 2009). In Sagami Bay, the SCM occurs near the thermocline in summer (Hashihama *et al*., 2008). In the present study, we found that the Chl *a* contributions of diatoms, prasinophytes and chlorophytes decreased during the time period 2.6–43.1 h (Fig. 4). Growth rates of these three phytoplankton groups were lower than those of other phytoplankters. In contrast, the Chl *a* contributions of cryptophytes increased over this time period, while those of haptophytes, dinoflagellates, and *Synechococcus* were largely stable (Fig. 4). The growth rates of cryptophytes and *Synechococcus* ($\mu = 1.11$ and 0.95 d^{-1}, respectively) estimated by Lagrangian observation were higher than those of pico- and nanoeukaryotes (Table 3). Slow growth rates, measured as Chl *a* (0.51 d^{-1}) may be attributable to the low growth activity in diatoms, which contributed at least 31% of Chl *a* standing stock.

Growth rates estimated for each phytoplankton group from Lagrangian observation were not significantly different from those from dilution experiment (A), except for nanoeukaryotes. Rates were about half the maximum growth rate of 1.96 d^{-1} that is expected in a discharged water at 19°C (Eppley *et al*., 1972). The growth rates we estimated by dilution cultures were within the range of reported values from dilution cultures of subsurface phytoplankton populations in subtropical regions (Table 4). Therefore, our growth rate estimates derived from Lagrangian observation are consistent with those of our shipboard incubations and with those of previous studies. Hence, we demonstrated active growth of cryptophytes and *Synechococcus* in the subsurface layer.

Growth rates of *Synechococcus* and cryptophytes obtained in culture experiment (B) for the sample collected at 42.9 h were significantly lower than those obtained in culture experiment (A). Consequently, growth rates of *Synechococcus*, picoeukaryotes, and cryptophytes estimated in culture experiment (B) were significantly lower than those obtained by Lagrangian observation. Because the sample collected for dilution experiment (B) at 42.9 h was considered to be under the influence of the Kyucho, which was originated from oligotrophic Kuroshio water, we likely made comparative observations on different algal populations with different growth activities in the two culture experiments.

Previous studies demonstrated that relief of nutrient limitation of surface populations by natural and artificial upwelling stimulates growth of diatoms (Ishizaka *et al*., 1983; Furuya *et al*., 1986; Aure *et al*., 2007). However, active diatom growth was not noted in the present study (Fig. 4), even though the concentration of nitrate in the discharged water exceeded 4.6 μM (Fig. 2). This observation implies that nutrients, at least nitrate, did not limit diatoms' growth. Why did they not grow actively despite sufficient nitrate availability? In other words, since we examined diatom growth by pigments, we can ask why pigment contents of diatoms were not elevated in the subsurface layer. Plausible explanations include (1) low light availabilty in the discharged water for diatom growth

during our observations (Nishikawa and Yamaguchi, 2008), (2) no observable increase of pigments in cells which was transported from 5-m depth to 20-m, and (3) longer lag-phase in diatoms' growth than that of picoeukaryotes and *Synechococcus* after relief of nutrient limitation (Mackey *et al*., 2009).

In the present study, evidence is not available to test these possibilities. However, as a matter of fact, diatom did not show any indication of growth enhancement. Although pigment contents of cells transported from 5-m depth by *Takumi* were expected to be elevated under much lower irradiance at 20-m depth, the absence of pigment increase in the present study is not contradictory to poor shade adaptation of surface originated populations. In contrast, during our experiments, cryptophytes and *Synechococcus*, which have the light harvesting phycobiliprotein, phycoerythrin, grew most actively (Table 1). Phycoerythrin contributes to photosynthesis by harvesting solar energy and transferring it to Chl *a* (French and Young, 1952). Cryptophytes are known to actively photosynthesize under low-light conditions (Spear-Bernstein and Miller, 1989). The initial slope of *Synechococcus* PE curve with photosynthetic rate measured on a unit Chl *a* basis suggests high photosynthetic efficiency at low light irradiances (MacIntyre *et al*., 2002). Hence, the active growth in the subsurface layer is, at least in part, attributable to high light utilization efficiency and high quantum yield resulting from chromatic adaptation of subsurface assemblages, i.e., efficient phycobiliprotein photon harvesting in the limited spectral range penetrating through to subsurface waters (Kishino *et al*., 1986; Moore *et al*., 2006; Hickman *et al*., 2009).

The present study is the first estimate of *in situ* phytoplankton growth rate in a subsurface layer. The active growth of pico- and nanophytoplankton was in a good agreement with bottle incubation experiments. We demonstrated active growth of pico- and nanophytoplankton, especially cryptophytes and *Synechococcus*, in the subsurface layer. Investigations focused on the effects of exogenous new nutrients on phytoplankton in subsurface layers are still needed to better understand if and how they will influence primary production and phytoplankton community structure in a stratified ocean. Furthermore, there is a need for better vertical resolution at finer scales for improving measurement of phytoplankton growth in subsurface waters.

Acknowledgements

We are grateful to Prof. Masayuki Mac Takahashi for his leadership in making the *Takumi* project run successfully. The project was financially supported by the Fisheries Agency, Japan. We thank Dr. Tohru Ikeya for providing uranine concentration data. We also wish to thank Prof. Paul J. Harrison for his comments on an earlier version of the manuscript. Thanks are due to the captain, crew and scientists on board the "Tansei-Maru" cruise.

References

Aure, J., O. Stand, S. R. Erga and T. Strohmeier (2007): Primary production enhancement by artificial upwelling in a western Norwegian fjord. *Mar. Ecol. Prog. Ser.*, **352**, 39–52.

Basterretxea, G., E. D. Barton, P. Tett, P. Sangrá, E. Navarro-Perez and J. Arístegui (2002): Eddy and deep chlorophyll maximum response to wind-shear in the lee of Gran Canaria. *Deep-Sea Res. I*, **49**, 1087–1101.

Boyd, P. W., T. Jickell, C. S. Law, S. Blain, E. A. Boyle, K. O. Buesseler, K. H. Coale, J. J. Cullen, H. J. W. de Baar, M. Follows, M. Harvey, C. Lancelot, M. Levasseur, N. P. J. Owens, R. Pollard, R. B. Rivkin, J. Sarmiento, V. Schoemann, V. Smetacek, S. Takeda, A. Tsuda, S. Turner and A. J. Watson (2007): Mesoscale iron enrichment experiments 1993–2005: Synthesis and future directions. *Science*, **315**, 612–617.

Cullen, J. J. and R. W. Eppley (1981): Chlorophyll maximum layers of the Southern Californian Bight and possible mechanisms of their formation and maintenance. *Oceanol. Acta*, **4**, 23–31.

Eppley, R. W. (1972): Temperature and phytoplankton growth in the sea. *Fish. Bull.*, **70**, 1063–1085.

Fischer, H. B., E. J. List, R. C. Y. Koh, J. Imberger and N. H. Brooks (1979): *Mixing in Inland and Coastal Waters*. Academic Press, New York, 483 pp.

French, C. S. and V. K. Young (1952): The fluorescence spectra of red algae and the transfer of energy from phycoerythrin to phycocyanin and chlorophyll. *J. Gen. Physiol.*, **35**, 873–890.

Furuya, K. (1990): Subsurface chlorophyll maximum in the tropical and subtropical western Pacific Ocean: vertical profiles of phytoplankton biomass and its relationship with chlorophyll *a* and particulate organic carbon. *Mar. Biol.*, **107**, 529–539.

Furuya, K. and R. Marumo (1983): The structure of the phytoplankton community in the subsurface chlorophyll maxima in the western North Pacific Ocean. *J. Plankton Res.*, **5**, 393–406.

Furuya, K., M. Takahashi and T. Nemoto (1986): Summer phytoplankton community structure and growth in a regional upwelling area off Hachijo Island, Japan. *J. Exp. Mar. Biol. Ecol.*, **96**, 43–55.

Hashihama, F., N. Horimoto, J. Kanda, K. Furuya, T. Ishimaru and T. Saino (2008): Temporal variation in phytoplankton composition related to water mass properties in the central part of Sagami bay. *J. Oceanogr.*, **64**, 23–37.

Hickman, A. E., P. M. Holligan, C. M. Moore, J. Sharples, V. Krivtsov and M. P. Palmer (2009): Distribution and chromatic adaptation of phytoplankton within a shelf sea thermocline. *Limnol. Oceanogr.*, **54**, 525–536.

Ikeya, T., N. Horimoto and Y. Kashino (2009): A practical method for sensitive determination of the fluorescent wa-

ter-tracer uranine by reversed phase HPLC under alkaline conditions. *Talanta*, doi:10.1016/j.talanta.2009.05.007.

Ishizaka, J., M. Takahashi and S. Ichimura (1983): Evaluation of coastal upwelling effects on phytoplankton growth by simulated culture experiments. *Mar. Biol.*, **76**, 271–278.

Kishino, M., N. Okami, M. Takahashi and S. Ichimura (1986): Light utilization efficiency and quantum yield of phytoplankton in a thermally stratified sea. *Limnol. Oceanogr.*, **31**, 557–566.

Landry, M. R. and R. P. Hassett (1982): Estimating the grazing impact of marine micro-zooplankton. *Mar. Biol.*, **67**, 283–288.

Landry, M. R., B. C. Monger and K. E. Selph (1993): Time-dependency of microzooplankton grazing and phytoplankton growth in the subarctic Pacific. *Prog. Oceanogr.*, **32**, 205–222.

Landry, M. R., J. Constantinou and J. Kirshtein (1995): Microzooplankton grazing in the central equatrial Pacific during February and August 1992. *Deep-Sea Res. II*, **42**, 657–671.

Landry, M. R., S. L. Brown, L. Campbell, J. Constantinou and H. Liu (1998): Spatial patterns in phytoplankton growth and microzooplankton grazing in the Arabian Sea during monsoon forcing. *Deep-Sea Res. II*, **45**, 2353–2368.

Landry, M. R., S. L. Brown, J. Neveux, C. Dupouy, J. Blanchot, S. Christensen and R. R. Bidigare (2003): Phytoplankton growth and microzooplankton grazing in high-nutrient, low-chlorophyll waters of the equatorial Pacific: Community and taxon-specific rate assessments from pigment and flow cytometric analyses. *J. Geophys. Res.*, **108**, doi:10.1029/2000JC000744.

MacIntyre, H. L., T. M. Kana, T. Anning and R. J. Geider (2002): Photoacclimation of photosynthesis irradiance response curves and photosynthetic pigments in microalgae and cyanobacteria. *J. Phycol.*, **38**, 17–38.

Mackey, K. R. M., T. Rivlin, A. R. Grossman, A. F. Post and A. Paytan (2009): Picophytoplankton responses to changing nutrient and light regimes during a bloom. *Mar. Biol.*, **156**, 1531–1546.

Mackey, M. D., D. J. Mackey, H. W. Higgins and S. W. Wright (1996): CHEMTAX-a program for estimating class abundance from chemical markers: application to HPLC measurements of phytoplankton. *Mar. Ecol. Prog. Ser.*, **144**, 265–283.

Mackey, M. D., D. J. Mackey, H. W. Higgins and S. W. Wright (1997): CHEMTAX User's Manual; a program for estimating class abundance from chemical markers-application to HPLC measurements of phytoplankton pigments. CSIRO Marine Laboratories Report 229, Hobart, Australia, 41 pp.

Mariano, J., A. Griffa, T. M. Özgökmen and E. Zambianchi (2002): Lagrangian analysis and predictability of coastal and ocean dynamics 2000. *J. Atmos. Oceanic Technol.*, **19**, 1114–1126.

Matsuyama, M., H. Ishidoya, S. Iwata, Y. Kitade and H. Nagamatsu (1999): Kyucho induced by intrusion of Kuroshio water in Sagami Bay, Japan. *Cont. Shelf Res.*, **19**, 1561–1575.

Miyabe, H., H. Kobayashi and S. Ogiwara (2004): Development of the floating structure for the ocean nutrient enhancer 'TAKUMI'. *Oceans '04. MTS/IEEE Techno-Ocean '04*, **1**, 348–353.

Moore, C. M., D. J. Suggett, A. E. Hickman, Y.-N. Kim, J. F. Tweddle, J. Sharples, R. J. Geider and P. M. Holligan (2006): Phytoplankton photoacclimation and photoadaptaion in response to environmental gradients in a shelf sea. *Limnol. Oceanogr.*, **51**, 936–949.

Nishikawa, T. and M. Yamaguchi (2008): Effect of temperature on light-limited growth of the harmful diatom *Coscinodiscus wailesii*, a causative organism in the bleaching of aquacultured *Porphyra thalli*. *Harmful Algae*, **7**, 561–566.

Obayashi, Y. and E. Tanoue (2002): Growth and mortality rates of phytoplankton in the northwestern North Pacific estimated by the dilution method and HPLC pigment analysis. *J. Exp. Mar. Biol. Ecol.*, **280**, 33–52.

Ouchi, K. and H. Omura (2004): Design concept and experiment of ocean nutrient enhancer 'TAKUMI'. *Oceans '04. MTS/IEEE Techno-Ocean '04*, **1**, 322–327.

Ouchi, K., K. Otsuka and H. Omura (2005): Resent advance of ocean nutrient enhancer 'TAKUMI' project. *Proc. of ISOPE Ocean Mining Symposium*, China Paper No. 2005-KO-01.

Parsons, T. R., M. Takahashi and B. Hargrave (1984): Photosynthesis and growth of phytoplankton in the sea. p. 87–99. In *Biological Oceanographic Processes 3rd edition*, ed. by T. R. Parsons, M. Takahashi and B. Hargrave, A. Wheaton and Co. Ltd., Oxford.

Richardson, K., A. W. Visser and F. B. Pedersen (2000): Subsurfacce phytoplankton blooms fuel pelagic production in the North Sea. *J. Plankton. Res.*, **22**, 1663–1671.

Riley, G. A. (1946): Factors controlling phytoplankton populations on Georges Bank. *J. Mar. Res.*, **6**, 54.

Ross, O. N. and J. Sharples (2007): Phytoplankton motility and the competition for nutrients in the thermocline. *Mar. Ecol. Prog. Ser.*, **347**, 21–38.

Ryther, J. H. (1969): Photosynthesis and fish production in the sea. *Science*, **166**, 72–77.

Saijo, Y., S. Iizuka and O. Asaoka (1969): Chlorophyll maximum in Kuroshio and adjacent area. *Mar. Biol.*, **4**, 190–196.

Selph, K. E., J. Shacat and M. R. Landry (2005): Microbial community composition and growth rates in the NW Pacific during spring 2002. *Geochem. Geophys. Geosyst.*, **6**, doi:10.1029/2005GC000983.

Sharples, J., C. M. Moore, T. P. Rippeth, P. M. Holligan, D. J. Hydes, N. R. Fisher and J. H. Simpson (2001): Phytoplankton distribution and survival in the thermocline. *Limnol. Oceanogr.*, **46**, 486–496.

Spear-Bernstein, L. and K. R. Miller (1989): Unique location of the phycobiliprotein light-harvesting pigment in the cryptophyceae. *J. Phycol.*, **25**, 412–419.

Suzuki, R. and T. Ishimaru (1990): An improved method for the determination of phytoplankton chlorophyll using N,N-dimethylformamide. *J. Oceanogr. Soc. Japan*, **46**, 190–194.

Takahashi, M. and T. Ikeya (2003): Ocean fertilization using deep ocean water (DOW). *Deep Ocean Res.*, **4**, 73–87.

Takahashi, M., K. Satake and N. Nakamoto (1972): Chlorophyll distribution and photosynthetic activity in the north and equatropical Pacific Ocean along 155°W. *J. Oceanogr.*

Soc. Japan, **28**, 27–34.
Takahashi, M., T. Nakai, T. Ishimaru, H. Hasumoto and Y. Fujita (1985): Distribution of the subsurface chlorophyll maximum and its nutrient-light environment in and around the Kuroshio off Japan. *J. Oceanogr. Soc. Japan*, **41**, 73–80.
Thingstad, T. F., M. D. Krom, R. F. C. Mantoura, G. A. F. Flaten, S. Groom, B. Herut, N. Kress, C. S. Law, A. Pasternak, P. Pitta, S. Psarra, F. Rassoulzadegan, T. Tanaka, A. Tselepides, P. Wassmann, E. M. S. Woodward, C. Wexels Riser, G. Zodiatis and T. Zohary (2005): Nature of phosphorus limitation in the ultraoligotrophic Eastern Mediterranean. *Science*, **309**, 1068–1071.
Venrick, E. L., J. R. Beers and J. F. Heinbokel (1977): A study of plankton dynamics and nutrient cycling in the central gyre of the North Pacific Ocean. *Limnol. Oceanogr.*, **18**, 534–551.
Weston, K., L. Fernand, D. K. Mills, R. Delahunty and J. Brown (2005): Primary production in the deep chlorophyll maximum of the central North Sea. *J. Plankton Res.*, **27**, 909–922.
Zapata, M., F. Rodrigues and J. L. Garrido (2000): Separation of chlorophylls and carotenoids from marine phytoplankton: a new HPLC method using a reversed phase C_8 culmun and pyridine-containing mobile phase. *Mar. Ecol. Prog. Ser.*, **195**, 29–45.